Near-bed turbulence and sediment flux measurements in tidal channels

S.A. Wright and D.R. Whealdon-Haught

U.S. Geological Survey, California Water Science Center, 6000 J Street, Placer Hall, Sacramento, CA 95819; PH (916)278-3024; email: sawright@usgs.gov

INTRODUCTION

Understanding the hydrodynamics and sediment transport dynamics in tidal channels is important for studies of estuary geomorphology, sediment supply to tidal wetlands, aquatic ecology and fish habitat, and dredging and navigation. Hydrodynamic and sediment transport data are essential for calibration and testing of numerical models that may be used to address management questions related to these topics. Herein we report preliminary analyses of near-bed turbulence and sediment flux measurements in the Sacramento-San Joaquin Delta, a large network of tidal channels and wetlands located at the confluence of the Sacramento and San Joaquin Rivers, California, USA (Figure 1). Measurements were made in 6 channels spanning a wide range of size and tidal conditions, from small channels that are primarily fluvial to large channels that are tidally dominated. The results of these measurements are summarized herein and the hydrodynamic and sediment transport characteristics of the channels are compared across this range of size and conditions.

METHODS

Measurements were made from a bottom-mounted frame and instrument package that was periodically moved between sites (Figure 1). The instrument package contained a Nortek Vector acoustic Doppler velocimeter (ADV), Sequoia Scientific LISST-100X laser diffraction particle sizer, and YSI multi-parameter sonde. Only data from the ADV are reported herein. Table 1 presents locations and ADV parameter settings for each deployment. Data were collected between March 2011 and March 2012. The length of deployment where useable data were retrieved ranged from 14 – 45 days (the wide range was due to biological fouling and frame movements). The ADV sampling rate varied from 8 to 32 Hz; however, subsampling of data collected at high sample rates indicated that rates as low as 1 Hz were adequate for computing turbulence quantities in these environments. Burst lengths were either 4 or 5 minutes; subsampling of these data indicated that burst lengths of >2 minutes maintain relative errors in turbulence quantities below 5% (as compared to the full burst length). The measurement volume of the ADV was approximately 45 cm above the bed for all deployments. Bursts were collected every 15 minutes at SMR, RY, and SRV, and every 30 minutes at the other 3 sites (Figure 1, different intervals were used due to testing power usage and requirements).

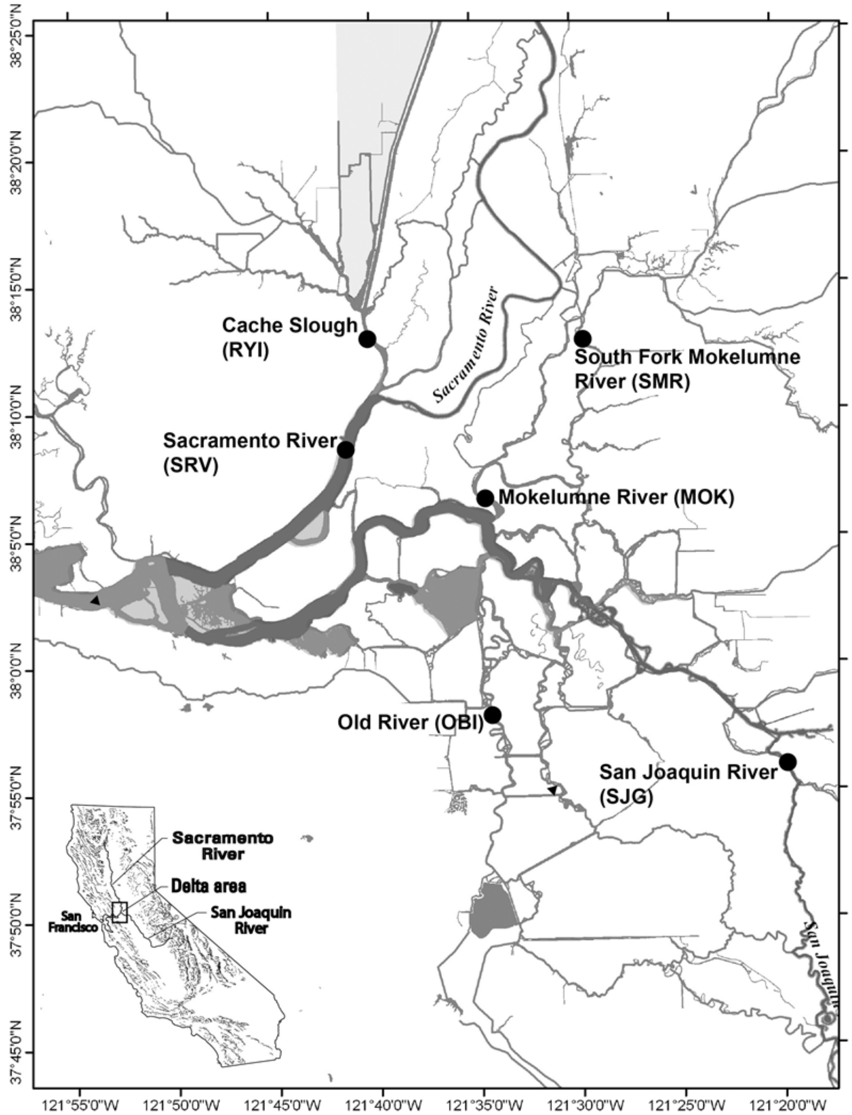

Figure 1. Map of the Sacramento-San Joaquin Delta showing data collection sites.

Table 1. Site locations and ADV deployment characteristics.

Site ID	USGS gage #	Latitude (N)	Longitude (W)	Start date	Length (days)	Sample rate (Hz)	Samples per burst
SMR	11336680	38°13'30.0"	121°29'28.3"	6/28/11	17	16	3840
SJG	11304810	37°56'07.8"	121°19'50.7"	5/11/11	35	32	9600
OBI	11313405	37°58'03.9"	121°34'27.3"	4/4/11	24	8	2400
MOK	11336930	38º06’29.9”	121º34’31.5”	3/1/11	14	32	9600
RYI	11455350	38º12’47.0”	121º40’04.5”	3/12/12	45	16	3840
SRV	11455420	38°08'54.2"	121°41'17.5"	2/14/12	27	16	3840

Table 2 summarizes the fluvial and tidal characteristics of the sites. The six sites can be roughly segregated into three groups based on channel size and flow characteristics (flows for the deployment periods detailed in Table 1 were obtained from http://cdec.water.ca.gov/). The two smallest channels, the south fork Mokelumne River (SMR) and San Joaquin River (SJG), experienced the lowest flows and the flows were primarily directed downstream. The medium-sized channels, Old River and the lower Mokelumne River, experienced larger flows with substantial flow reversals. The two largest channels, Cache Slough (RYI) and the Sacramento River (SRV), had by far the largest flows and were primarily tidal with ebb and flood flows of approximately equal magnitude. All sites experienced stage variations of approximately one meter due to tides.

Table 2. Channel size, flow, and depth characteristics of the deployment sites. Positive flows are ebb-directed, negative flows are flood-directed.

Site ID	Channel width (m)	Mean Q (cms)	Mean unsigned Q (cms)[1]	95% exceeded Q (cms)	5% exceeded Q (cms)	Mean depth[2] (m)	Depth range (m)
SMR	50	32	32	0.8	55	3.6	0.90
SJG	60	150	150	90	190	6.5	0.94
OBI	170	100	240	-280	380	10.5	0.88
MOK	190	200	290	-240	530	7.5	0.81
RYI	270	610	2,100	-2,800	3,800	11.0	1.0
SRV	690	250	2,100	-3,100	3,300	6.8	1.1

[1]mean unsigned Q is the mean flow following taking the absolute value
[2]depths are from a built-in pressure transducer on the ADV

Time-averaged data and turbulence quantities were computed using standard Reynolds decomposition of the burst data, as follows:

$$\tau/\rho = -\overline{u'w'} = -\overline{(u-\bar{u})(w-\bar{w})} \quad (1)$$

$$F_t = \overline{w'c'} = \overline{(w-\bar{w})(c-\bar{c})} \quad (2)$$

where τ/ρ represents the near-bed shear stress, u, $\bar{u}$, and u' are the instantaneous, time-averaged, and turbulent velocities, respectively, in the streamwise direction (positive downstream); w, $\bar{w}$, and w' are the instantaneous, time-averaged, and turbulent velocities, respectively, in the vertical direction (positive upward); c, $\bar{c}$, and c' are the instantaneous, time-averaged, and turbulent sediment concentrations, respectively; F_t represents the near-bed vertical turbulent sediment flux. Overbars denote time averages of burst data. For the analyses presented herein, acoustic backscatter from the ADV (signal-to-noise ratio, SNR, in decibels, dB) was used to represent sediment concentrations. Comparison of SNR with concurrent turbidity data indicated high probabilities of correlation (all p-values << 0.001) but with significant scatter likely due to variable particle size and density at the sites (flocculation occurs at all sites based on preliminary LISST-100X data). Because we are only using the turbulent fluctuating component of SNR in our calculations (eq. 2), differences in mean SNR between sites due to particle characteristics may not be critically important. However, more definitive analyses of the interrelations between SNR, turbidity, particle size and density are ongoing and await processing of sediment samples and LISST-100X data. Velocity and shear stress vectors were rotated from instrument-derived east/north coordinates to streamwise and lateral components. Plots of time-averaged velocity and shear stress direction were used to estimate the streamwise (and thus lateral) directions of velocity and shear stress (separately). Only the streamwise components are presented herein. It is noted that the streamwise direction of velocity and shear stress were not always equivalent. At five of the sites the offsets were small, ranging from 5 to 20 degrees, whereas the offset at SJG was almost 90 degrees likely due to the deployment site being in the outside of a bend.

Two coefficients were defined and evaluated to compare the hydrodynamic and sediment transport characteristics between sites:

	$C_D = -\overline{u'w'}/u^2$	(3)
	$C_S = \overline{w'c'}/\sqrt{-u'w'}$	(4)

The drag coefficient, C_D, is an indication of the resistance to flow in a channel, i.e., it controls the velocity magnitude that results for a given shear stress. The sediment coefficient, C_S, is an indication of the amount of vertical turbulent sediment flux that occurs for a given shear stress. C_D and C_S were computed for each measurement and median values were calculated (to avoid bias by eliminating spikes during very low velocity and stress at slack tide) for ebb and flood tides for each site.

RESULTS AND DISCUSSION

The data and calculation results are presented in Figure 2-6. Boxplots are used in order to present all of the data in a concise format.

Figures 2 and 3 show the measured streamwise velocities and computed shear stresses (eq. 1) at the six sites. A clear increase in variability due to tides was seen in velocity between the more fluvial sites (SMR, SJG, Figure 2) and the sites which are primarily tidal (RYI, SRV). All sites have ebb-directed mean velocity (positive values), as expected. However, it is noteworthy that the highest velocities were comparable at all sites (~0.5 m/s). In contrast, shear stress (Figure 3) was highest in the more fluvial reaches (SMR, SJG) with a general decrease in the downstream direction to the tidally-dominated sites. Similar to velocity, flood-directed shear stress (negative values) is greatest in the dominantly tidal sites (RYI, SRV) such that an approximate balance between ebb and flood shear stress develops. Figure 4 shows the computed drag coefficients (eq. 3) for ebb and flood tides. Greater ebb tide drag coefficients were observed at the fluvial sites compared to the tidal sites, with the highest drag coefficients at SMR and SJG. For the primarily tidal sites, the computed drag coefficients are comparable on ebb and flood tides, whereas a substantial ebb-flood imbalance was measured at SMR (SJG typically has reversing flow but did not during our deployment period due to high upstream river flows). One interpretation is that the fluvial sites have bedform shapes that are skewed in the ebb direction, resulting in increased drag on flood tides, whereas the tidal sites have bedforms that are not skewed in either direction (or no bedforms). However, this result is based solely on the SMR site; work is ongoing to further evaluate this result.

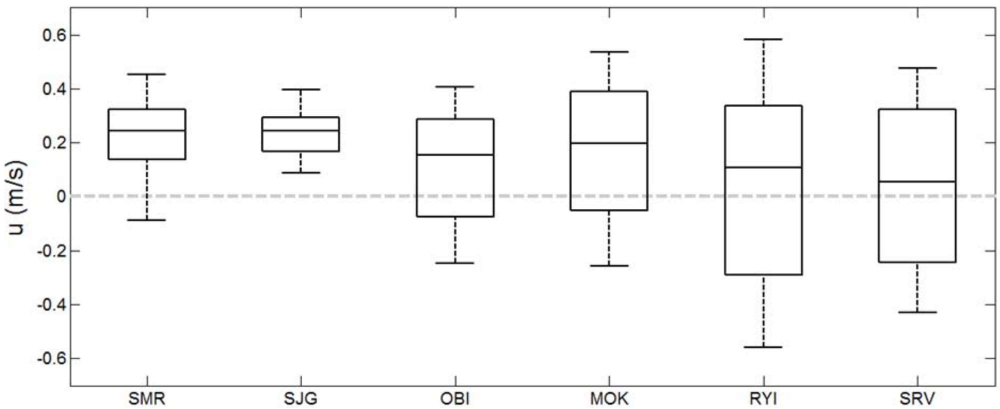

Figure 2. Summary of streamwise velocity data at deployment sites (Figure 1)

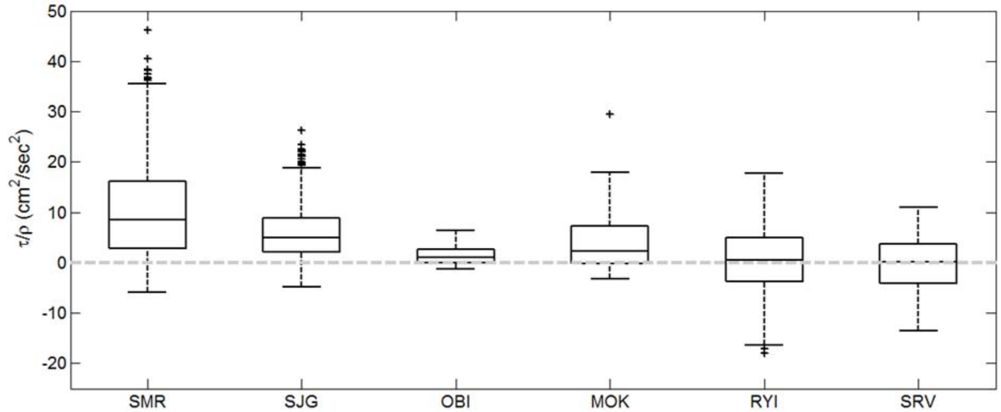

Figure 3. Summary of streamwise shear stress calculations.

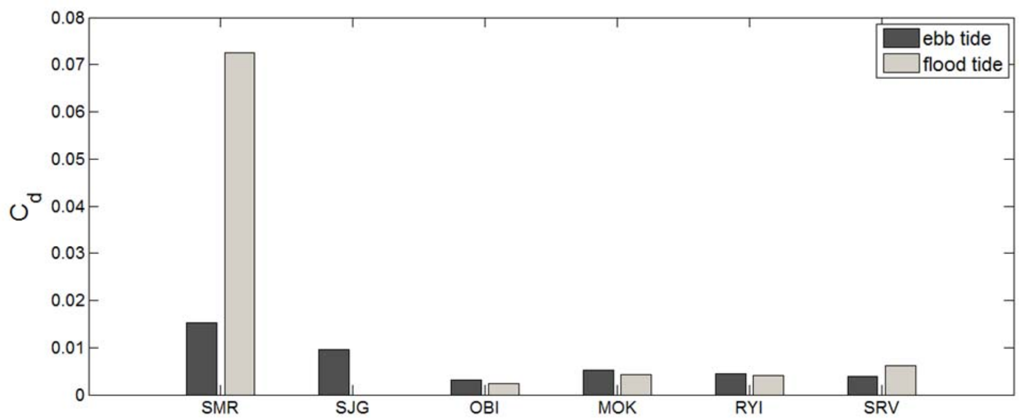

Figure 4. Median drag coefficients for flood and ebb tide.

Figure 5 shows the results of the calculations of the vertical turbulent suspended-sediment flux, F_t (eq. 2). Comparisons between sites must be done with caution because, as detailed in the Methods section, acoustic backscatter (SNR) was used in place of sediment concentration for this preliminary analysis. Turbulent sediment fluxes were almost exclusively in the upward direction, indicating that positive vertical velocities are correlated with positive fluctuations in backscatter. This lends support to this method because it agrees with the fundamental of suspended-sediment transport theory, i.e. upward turbulent sediment flux is balanced by downward settling. The calculations suggest that the Mokelumne River sites (SMR and MOK) experienced a wider range of vertical sediment fluxes (Figure 5). Figure 6 shows calculations of the sediment flux scaled by the shear stress (sediment coefficient, eq. 4), for ebb and flood tide. A general trend emerges from these calculations that three of the sites (SMR, OBI, and MOK) exhibit a substantial imbalance between ebb and flood sediment coefficients, whereas two sites (RYI and SRV) show very little imbalance. One interpretation of this result is related to the proximity of a site to sediment sources. The three sites with the ebb-flood imbalance are located further upstream and closer to the fluvial sediment sources from the watershed, whereas the two balanced sites are located at the downstream end of the Delta and within a tidal excursion of Suisun Bay, a potentially large source of fine sediment during flood tides. More definitive analyses await processing of suspended and bed sediment samples as well as *in situ* particle size data.

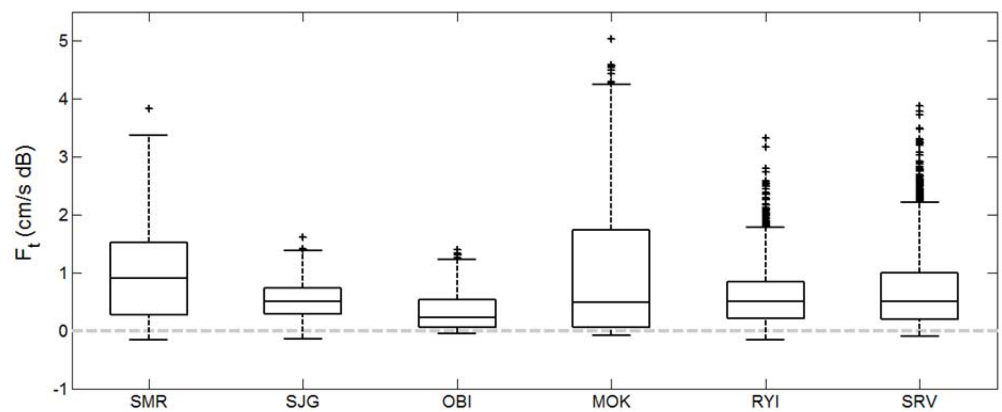

Figure 5. Summary of turbulent sediment flux calculations.

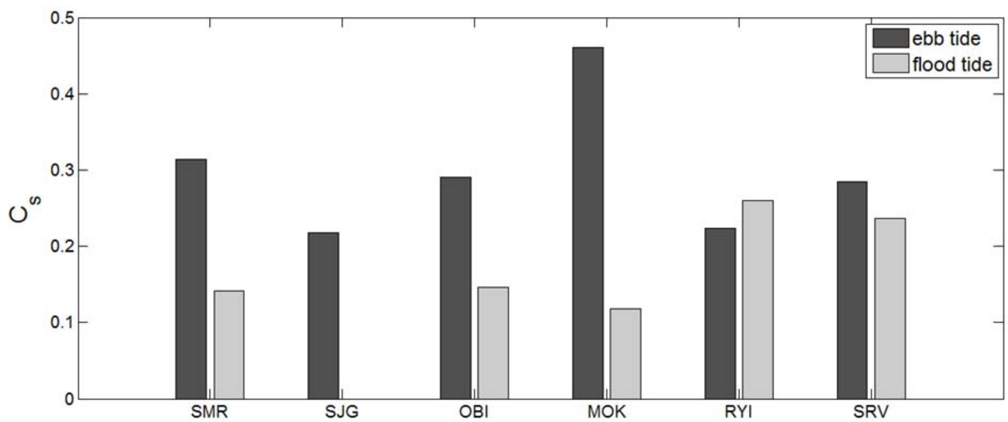

Figure 6. Median sediment coefficients for flood and ebb tide.